Computer Modeling of Heat Flow in Welds

J. GOLDAK, M. BIBBY, J. MOORE, R. HOUSE, and B. PATEL

This paper summarizes progress in the development of methods, models, and software for analyzing or simulating the flow of heat in welds as realistically and accurately as possible. First the fundamental equations for heat transfer are presented and then a formulation for a nonlinear transient finite element analysis (FEA) to solve them is described. Next the magnetohydrodynamics of the arc and the fluid mechanics of the weld pool are approximated by a flux or power density distribution selected to predict the temperature field as accurately as possible. To assess the accuracy of a model, the computed and experimentally determined fusion zone boundaries are compared. For arc welds, accurate results are obtained with a power density distribution in which surfaces of constant power density are ellipsoids and on radial lines the power density obeys a Gaussian distribution. Three dimensional, in-plane and cross-sectional kinematic models for heat flow are defined. Guidelines for spatial and time discretization are discussed. The FEA computed and experimentally measured temperature field, $T(x, y, z, t)$, for several welding situations is used to demonstrate the effect of temperature dependent thermal properties, radiation, convection, and the distribution of energy in the arc.

I. INTRODUCTION

FUSION welding is the method of choice for assembling most large metal structures such as ships, bridges, nuclear reactors, pipelines, trains, and cars. In these structures safety and economy are important issues. In simple terms, a fusion weld is produced by moving a localized intense heat source along the joint. The chemical composition of the weld metal, energy, and position of the arc must be carefully controlled to achieve the desired weld quality. Often filler metal is added. This complex process that mimics the entire steelmaking process in a volume of roughly one cubic cm in a time span of less than one minute has largely been developed by experiment, *i.e.*, trial and error. The process is so complex that to date mathematical modeling has contributed little to modern welding technology. This presentation argues that recent developments in computational weld mechanics now enable the heat transfer in real welding situations to be analyzed or simulated accurately, perhaps more accurately than the data can be measured.

The critical first step in an accurate analysis of the physical behavior of welds is to compute the transient temperature field, $T(x, y, z, t)$, for any point of interest, (x, y, z), and for any instant of time, t. For a given material and joint design, this temperature field largely determines the size of the fusion zone and heat-affected zone, the microstructure, residual stress, distortion, hydrogen content, and it is fundamental to understanding and analyzing weld defects. For a range of materials and joint designs, the temperature field, together with the chemical composition and transformation kinetics, is the basis for predicting the microstructure in the FZ and HAZ. In determining the residual strain and stress, the temperature dependent stress-strain relationship also plays an important role. In short, any computer simulation of these topics depends on and is sensitive to the accuracy of the computed temperature field.

In particular, the heat source generates a transient temperature field that has important consequences. It modifies the microstructure by solidification, recrystallization, grain growth, and phase transformations such as ferrite to austenite to martensite. The microstructure controls the thermal and mechanical properties of the weldment. The transient temperature field causes thermal expansion, stress, and strain that usually plastically deforms in the weld neighborhood and results in residual stress and strain; *i.e.*, when the weldment cools a stress remains and the structure is distorted from its original shape.

Distortion is the bane of fabricators because it increases their costs and delays production. It is managed by a variety of techniques including balanced welds, rigid fixturing, and preweld distortion. Indeed, flame straightening and flame bending use localized heating to distort structures into desirable shapes. To date, this is done empirically in most cases.

Residual stresses affect the in-service performance of welded structures. In particular, low temperature brittle fracture, fatigue, stress corrosion cracking, and buckling can be significantly aggravated by residual stresses in weldments. In many structures, thermal stress relief is not feasible. If it is feasible, it is expensive.

For more than a decade the goal of the authors' laboratory has been to develop a rigorous methodology, models, and software to analyze accurately and realistically welding processes and welded structures. A high priority has been given to building upon the fundamental laws of continuum mechanics. *Ad hoc* empirical procedures were discouraged from the outset because they have little long term value. The complexity of the phenomena are such that they can be managed only by computerization. Nonlinear transient finite element analysis provided an ideal numerical method for solving the equations of continuum mechanics for the complex geometries of welded structures, the temperature and history dependent constitutive equations, and the complex boundary conditions associated with welding arcs. The software was to be extensible in order to grow as new knowledge became available. Users were to be shielded from procedures and data structures that need not concern them.

This project is unique in that a rather general purpose finite element analysis code is being developed specifically for the analysis of welds and welded structures. It draws

J. GOLDAK and M. BIBBY, Professors, and J. MOORE, R. HOUSE, and B. PATEL, Graduate Students, are with the Department of Mechanical and Aeronautical Engineering, Carleton University, Ottawa, ON, Canada, K1S 5B6.

Manuscript submitted May 24, 1985.

upon continuum mechanics, finite element analysis, computer science, welding, metallurgical and mechanical technology. The heat transfer theory, numerical method, and models are described in the following sections and to demonstrate the capability of the system, computed temperature fields for several steel and aluminum weldments are analyzed and compared with experiment.

II. THEORY

A. *The Heat Equation*

The temperature, $T(x, y, z, t)$, as a function of spatial coordinates, (x, y, z), and time, t, satisfies the following parabolic differential equation, the heat equation, at every point in the domain, Ω:

$$\frac{\partial}{\partial x}k_x\frac{\partial T}{\partial x} + \frac{\partial}{\partial y}k_y\frac{\partial T}{\partial y} + \frac{\partial}{\partial z}k_z\frac{\partial T}{\partial z} + Q = c\frac{\partial T}{\partial t} \quad [1]$$

$Q(x, y, z, t)$ = source or sink rate of heat in Ω (W/m^3)
k = thermal conductivity (W/mC)
c = volumetric specific heat (J/m^{3}C)

If k or c are functions of T, Eq. [1] is nonlinear.

On the boundary of Ω either the essential or natural boundary conditions must be satisfied. The essential boundary condition can be defined as:

$$T(x, y, z, t) = T_1(x, y, z, t) \text{ on the boundary } S_1; \quad i.e., (x, y, z) \in S_1 : t > 0 \quad [2]$$

The natural boundary condition can be defined as:

$$k_n\frac{\partial T}{\partial n} + q + \alpha(T - T_0) + \sigma\varepsilon(T^4 - T_0^4) = 0 \quad [3]$$

on the boundary S_2; *i.e.*, $(x, y, z) \in S_2 : t > 0$.

k_n = thermal conductivity normal to the surface (W/mC)
$q(x, y, z, t)$ = a prescribed flux (W/m^2)
α = heat transfer coefficient for convection (W/m^{2}C)
σ = Stefan-Boltzmann constant (W/m^{2}C^4)
ε = emissivity
T_0 = the ambient temperature for convection and/or radiation (C).

If radiation is included or if the convective heat transfer coefficient is temperature dependent, this boundary condition is nonlinear.

In addition, the initial condition must be specified for $(x, y, z) \in \Omega$:

$$T(x, y, z, 0) = T_0(x, y, z) \quad [4]$$

If the partial differential Eq. [1], the boundary conditions [2] and [3], and the initial condition [4] are consistent, the problem is well posed and a unique solution exists.

B. *Finite Element Formulation for Transient Heat Flow*

Of the three strong candidate numerical methods, finite difference, boundary element, and finite element analysis, the authors have chosen the finite element method for several reasons. It has the best capability for nonlinear analysis and dealing with complex geometry. In addition, it is the most compatible with modern integrated CAD/CAM software systems. For thermal analysis alone, a strong argument can be made in favor of finite difference methods. However, for thermo-elasto-plastic analysis the argument is stronger for finite element analysis. The boundary element method is not well developed for nonlinear analysis. However, none of the above arguments is compelling and any of these methods can be used. The background and preferences of the developer are probably the deciding factor. In any case, developing a code with the power and functionality needed to analyze real problems requires many man years of effort by experts. Thus the choice of method is a major task quite beyond the scope of this paper. The authors' experience is with finite element analysis and all subsequent work will refer to this method.

The basis of the finite element method (FEM) is a piecewise polynomial approximation for the temperature field within each element:

$$T(x, y, z, t) = \sum_{i=1}^{\text{nodes}} N_i(x, y, z)T_i(t) \quad [5]$$

where N_i are basis functions dependent only on the type of element and its size and shape. Physically, $T_i(t)$ are the nodal values of the temperature at time t. Mathematically, they are undetermined coefficients. The analyst specifies the basis functions N_i by creating a mesh which in turn determines the type and position of each element. In the authors' program, more than one hundred types of elements are available. Four and eight node quadrilaterals, six node triangles, twenty and eight node brick elements are most frequently used.

The temperature gradient at any point (x, y, z, t) can be computed directly from Eq. [5]:

$$\left[\frac{\partial T}{\partial x}, \frac{\partial T}{\partial y}, \frac{\partial T}{\partial z}\right] = \left[\frac{\partial N_i}{\partial x}T_i, \frac{\partial N_i}{\partial y}T_i, \frac{\partial N_i}{\partial z}T_i\right] \quad [6]$$

where $\Sigma N_i(x, y, z)T_i(t)$ is abbreviated to N_iT_i.

The next question is how to evaluate T_i? Galerkin's FEM is among the most convenient and general of the methods available for this purpose. If Eq. [5] is substituted into Eq. [1], a residual or error term must be added. If this was not true, Eq. [5] would be the exact solution. Indeed, when Eq. [5] is the exact solution, the error in the FEM is zero.

Galerkin's FEM requires:

$$\int_\Omega \varepsilon N_i \, d\Omega = 0 \quad [7]$$

Mathematically, N_i in Eq. [7] is a test function and the N_i terms in Eq. [5] are the trial functions. Since there are i nodes, Eq. [7] creates a set of i ordinary differential equations which are integrated to form a set of nonlinear algebraic equations:

$$[K][T] = [R] \quad [8]$$

where $[K]$ is an effective conductivity or stiffness matrix and $[R]$ is an effective load or residual vector. Briefly, if each node is fixed at temperature $[T]$, a thermal load of magnitude $[R]$ (w) must be applied at each node. These are solved for the nodal temperatures T_i. The authors use various forms of a Newton-Raphson method together with a Gaussian elimination and back substitution direct solver as described in Reference 24.

C. *Models for Welding Heat Sources*

Rykalin's review[1] summarized current knowledge of heat sources for welds. The basic facts are that weld heat sources produce high heat fluxes which range from 10^4 to 2×10^4 kJ/mm^2 for arc sources to 10^8 kJ/mm^2 or higher for focused electron and laser beams. The flux is brightest at the center, and in most cases measurements of stationary sources suggest a Gaussian energy distribution. While the distribution for moving arcs has not been specifically measured, pictures suggest that the Gaussian distribution is probably skewed toward the trailing edge.[2] This could result from an arc/anode interaction. Gas velocities and current densities in the plasma are high. The surface of the weld pool is depressed. In plasma, laser, and electron beam welds, the depression often penetrates the plate to form a keyhole. The molten zone is stirred intensively. A rigorous analysis of the heat source for solving the magnetohydrodynamics of the arc and the fluid mechanics of the molten zone is some years away. The most comprehensive review of the physics of the arc and the molten pool is Lancaster's book.[2] The model proposed by Dilawari, Eagar, and Szekely[3,4] for stirring in electroslag welds is a notable advance. Lawson and Kerr[5] studied stirring and mixing effects in TIG welds. While studies such as the above are important steps toward developing rigorous models for heat sources, it is not yet possible to predict the size and shape of the molten pool from weld process parameters such as current, voltage, speed, electrode size, shape and attitude, *etc.* Current weld analysis assumes simpler models that do not explicitly incorporate stirring in the weld pool or the digging of the arc to depress the weld pool surface. In the best of these models, the size and shape of the molten pool is taken as data. This capability of computing accurate temperature fields, which is the essential first step in computing accurate microstructures and residual stress and strain fields in realistic welds, is the justification for creating these models. The authors know of no empirical formulae that are capable of computing temperature fields with comparable accuracy in realistic welds.

The analyst's knowledge of the heat source can be summarized as follows. The values of the welding parameters of current, voltage, and speed are known. The geometry of the weldment is known. The materials properties are either known or must be estimated. This is often a serious limitation because in many cases high temperature properties have not been published (see Section II–J for further discussion).

The fusion zone and HAZ boundaries represent known isotherms that can be measured from a micrograph of a weld cross-section. Thermocouples can be placed in the HAZ or plunged into the molten zone to record the thermal cycle at a number of points. Of course, these data are not known exactly but only within experimental error. The analyst requires a heat source model that accurately predicts the temperature field, $T(x, y, z, t)$, in the weldment.

Rosenthal[6] and Rykalin[1] proposed point, line, and plane models that are particularly convenient for classical closed form analysis (Figure 1). Myers *et al.*[7] reviewed this subject in depth. Closed form solutions suffer from several weaknesses. The geometry is usually highly idealized into forms such as infinite plates or bars. The thermal properties and boundary conditions are usually set equal to a constant

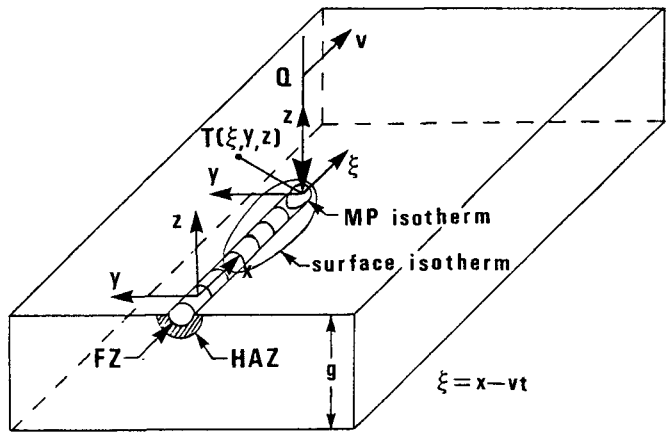

$$T(\xi, y, z) = T_o + \frac{\dot{Q}}{2\pi k} \exp\left(-\frac{v\xi}{2\lambda}\right)\left\{\sum_{n=-\infty}^{\infty} \frac{1}{R_n} \exp\left(-\frac{vR_n}{2\lambda}\right)\right\}$$

$$R_n = \sqrt{\xi^2 + y^2 + (z \pm 2ng)^2}$$

$$\xi = x - vt$$

Fig. 1—An idealized point source moving along the surface of a workpiece used for computing the transient temperature fields, $T(x, y, z, t)$, with the classical closed form analytical solutions of Rosenthal/Rykalin.[6,1] T_0 is the ambient temperature (°C), t is time (s), Q is the heat input rate (W); where $Q = \eta VI$. V is voltage, I is current, and η is the process efficiency; k is thermal conductivity (W/m °C), λ is thermal diffusivity (m^2/s), v is the welding speed (m/s); (x, y, z) is a fixed axes system and (ξ, y, z) is an axes system that moves with the heat source, n is an integer, MP is the melting point temperature which in turn is used to define the fusion zone (FZ), and HAZ is the heat-affected zone.

value. Convection and radiation are usually ignored. The point, line, and plane sources idealize a heat source which in reality is distributed. These solutions are most accurate far from the heat source. At the source, the error in temperature is large—sometimes even infinite! Near the heat source the accuracy can be improved by matching the theoretical solution to experimental data. This is usually done by choosing a fictitious thermal conductivity value.

With numerical methods, these deficiencies have been corrected and more realistic models that are just as rigorous mathematically have been developed. Temperature dependent thermal conductivity and heat capacity can be taken into account (Figures 2 and 3 for low carbon steels). In addition, temperature dependent convection and radiation coefficients can be applied to the boundaries. Contact thermal resistance between the plate and the fixturing can be incorporated. Perhaps the most important factor is to distribute the heat rather than assume point or line sources.

One of the earliest models due to Westby[8] assumed that the weld energy was distributed throughout the molten zone with a constant power density. A similar heat source configuration was used by Paley.[9] Experimental evidence shows clearly that the energy is not uniformly distributed. Pavelic[10] distributed the energy in a circular disc with a Gaussian flux distribution on the surface of the workpiece. This is realistic for preheating situations in which there is no melting but ignores the digging effect of the welding arc in distributing

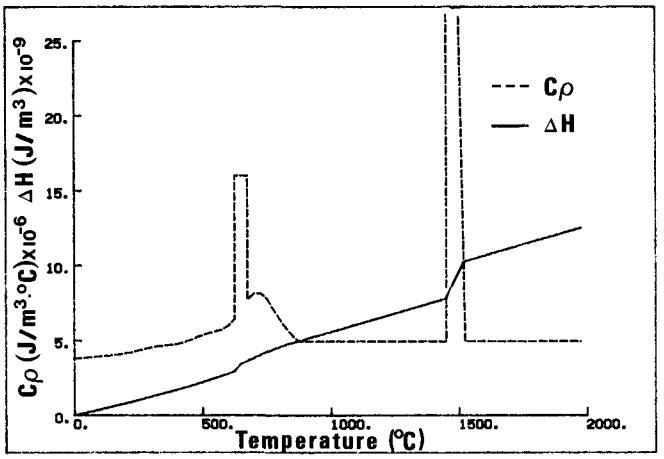

Fig. 2—The volumetric heat capacity and latent heats of fusion and transformation for low carbon steels as a function of temperature. In addition, the enthalpy-temperature relationship.

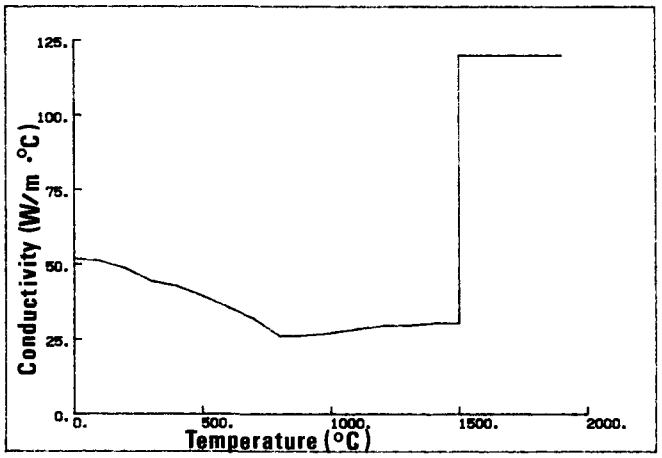

Fig. 3—The thermal conductivity of low carbon steels as a function of temperature. Note that a high conductivity in the molten region is used to simulate heat transfer by stirring.

the energy. Kou[11] also used both Gaussian and constant flux distributions in a circular disc on the surface of the weld. Argyris, Szimmat, and Willan[12] prescribed the temperature in the molten zone. However, it is not clear which of the following methods they used. The temperature of the molten pool was set equal to the melting temperature, the temperature of the FZ/HAZ boundary was set equal to the melting temperature, or a temperature distribution was assumed for the molten zone that was a maximum at the center and decayed to the melting temperature at the FZ boundary. The latter is the most realistic and preferable mathematically. The first two options introduce discontinuities in the temperature field which are unrealistic and mathematically undesirable. Since the temperature distribution in the molten zone is not constant except in the steady state, these models do not permit the analysis of transients during weld start, stop, run-on, or run-off situations where the size and shape of the molten pool must change.

The most realistic models developed to date are due to Goldak *et al.*[13] In these models arbitrary functions are used to define the distribution of flux on the surface of the weld and the power density throughout the volume of the weld. For arc welds, a double elliptical disc with a Gaussian distri bution of flux on the surface of the weld, together with one double ellipsoid function with a Gaussian distribution o power density to model the direct impingement of the arc and a second double ellipsoid with Gaussian distribution tc model the energy distributed by stirring the molten metal ha: given the most accurate temperature fields computed to date (Figure 4). In cases where the fusion zone differs from the ellipsoidal shape, other models should be used for the flu: and power density distribution. For example, in welds with a cross-section shaped as shown in Figure 5, four ellipsoic quadrants can be superimposed to model more accurately such welds. For deep penetration electron and laser beam welds, a conical distribution of power density which has a Gaussian distribution radially and a linear distribution axially has yielded the most accurate results (Figure 6(a)). The analyst must specify these functions or at least the parame ters such as weld current, voltage, speed, arc efficiency, anc the size and position of the discs, ellipsoids, and/or cones In some cases the weld pool size and shape can be estimatec from cross-sectional metallographic data and from surface ripple markings. If such data are not available, the methoc for estimating the weld pool dimensions suggested by Christensen[14] for arc welds and by Bibby *et al.*[15] for deep penetration electron beam or laser welds should be used

The size and shape of the heat source model is fixed by the ellipsoid parameters defined in Figure 4. Good agree ment between actual and computed weld pool size is ob tained if the size selected is about 10 pct smaller than the actual weld pool size. If the ellipsoid semi-axes are too long the peak temperature is too low and the fusion zone too small. The authors' experience is that accurate results ar obtained when the computed weld pool dimensions ar slightly larger than the ellipsoid dimensions. This is easily achieved in a few iterations. Chakravarti and Goldak[16] hav studied the sensitivity of the temperature field to the ellip soid parameters.

On the one hand, these distribution functions can be criti cized as 'fudge' factors. On the other hand, they do enabl accurate temperature fields to be computed. Chosen wisely varying any parameter changes the computed temperatur field. It can be argued that they are needed to model th many complex effects that are quantitatively known, such a electrode angle, arc length, joint design, and shielding ga composition.[17] Since they allow the analyst to compute ac curately the temperature field in weldments, they are to b preferred until better models are developed.

The addition of filler metal poses an interesting problem The simplest solution is to assume that the filler metal is i place at the start of the analysis. This is the authors' usu: practice and is expected to model the region that is coolin quite accurately but leads to obvious errors in a small regio immediately ahead of the weld pool. It is also possible t add filler by adding elements or changing nodal coordinate during the analysis. Since it is necessary to conserve energy the analyst must specify the initial temperature of the meta added. If it is hot, the energy of the heat source should b reduced because arc efficiency presumably includes th energy added with the filler metal. The authors have con ducted some preliminary analyses, but much more researc is needed to develop effective models for the addition c filler metal.

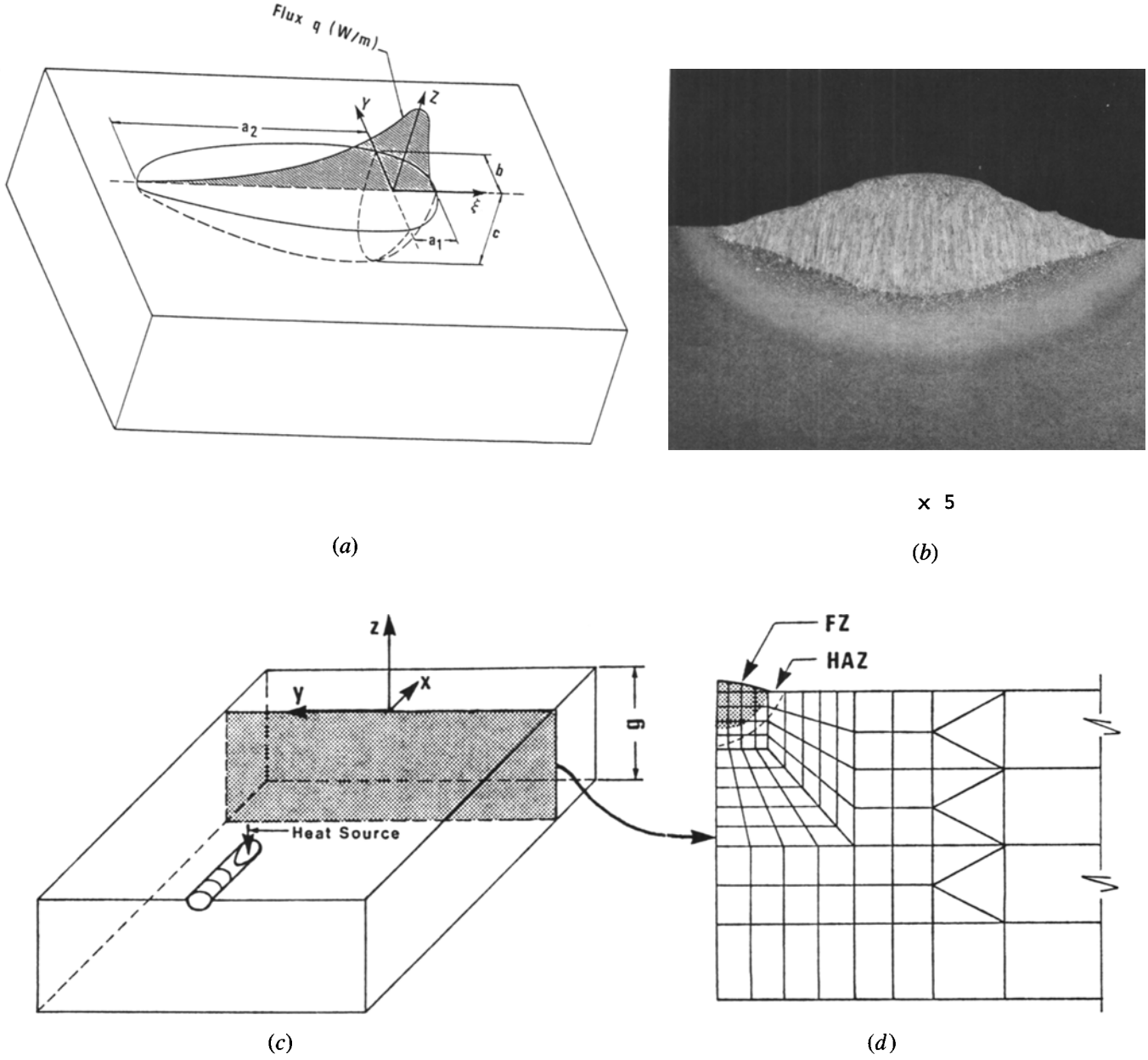

Fig. 4 — FEA weld analysis: (*a*) double ellipsoid heat source model, (*b*) cross-section of an SMAW weld bead on a thick plate of low carbon steel (V = 30 volts, I = 265 amps, v = 3.8 mm/s, g = 38 mm, T_0 = 20.5 °C), (*c*) reference plane concept, and (*d*) mesh used for the analysis.

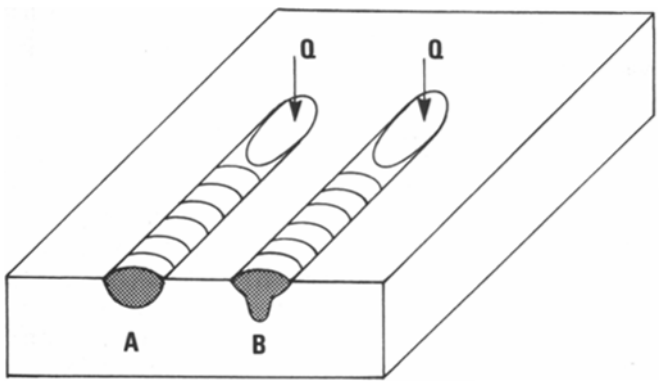

Fig. 5 — Cross-sectional weld shape of the fusion zone where (A) a double ellipsoid is used to approximate the heat source, (B) compound double ellipsoids must be used where there is a "hot top" nail head configuration.

D. *Kinematic Models for Heat Transfer in Welds*

Having selected a model for the heat source, the analyst has the option of assuming the heat flows only in cross-sectional planes, only in the plane of the plate or is free to flow in all three dimensions. Such assumptions are analogous to those applied to the displacement field in beams, plates, and shells in structural analysis. Since the assumptions restrict the orientation of the thermal gradient, it is suggested they be called kinematic models. Of course, these kinematic models are quite distinct from the heat source models described in the previous section. In choosing a kinematic model, the analyst must balance accuracy against cost. In all cases, reality is three dimensional but the cost of analysis is the highest. Constraining heat flow to the plane of the plate can achieve useful accuracy for thin plates, particularly with deep penetration plasma, electron, and

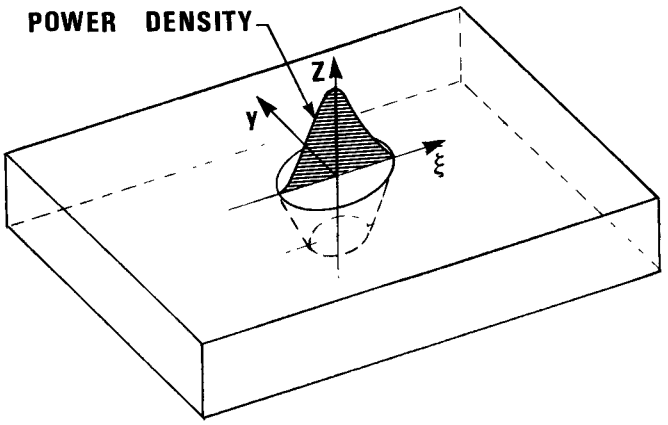

(a)

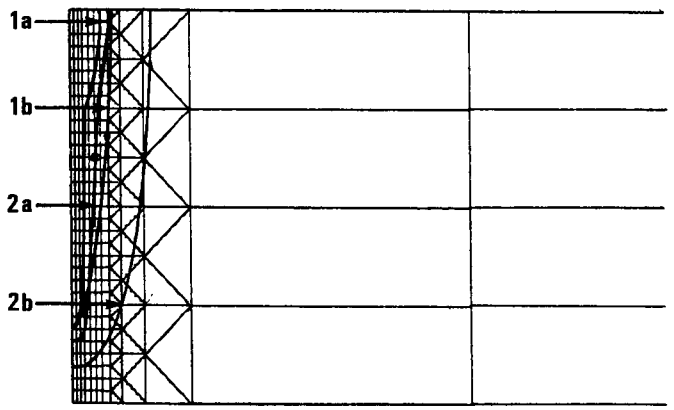

(b)

(1a) FZ —Experimental
(1b) FZ —Analytic (FEM)
(2a) HAZ—Experimental
(2b) HAZ—Analytic (FEM)

Fig. 6—A conical weld heat source used for analyzing deep penetration electron beam or laser welds: (*a*) conical source, (*b*) computed and measured FZ and HAZ boundaries. (V = 70 kV, I = 40 mA, v = 4.23 mm/s, g = 12.7 mm, T_0 = 21 °C).

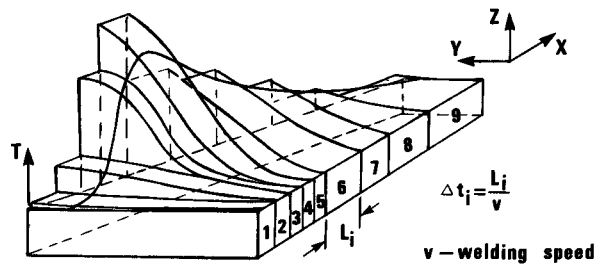

(a)

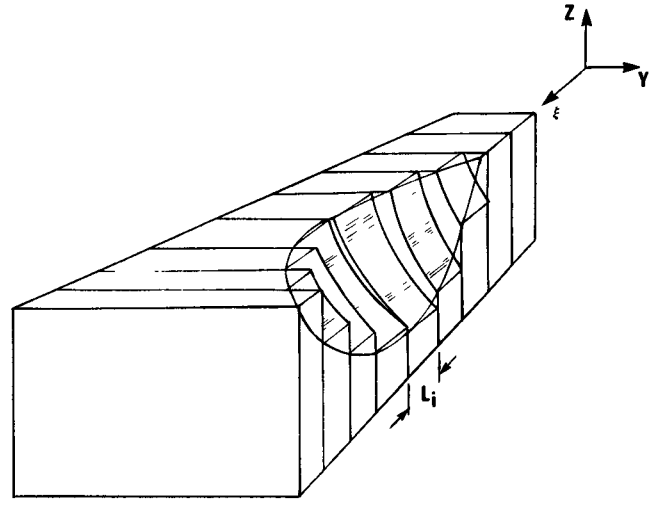

(b)

Fig. 7—(*a*) For the cross-sectional model, the temperature distribution or a series of slices to show the temperature field at several instants in time (*b*) approximate 3D steady state FZ boundary obtained from the cross sectional model.

laser beam welds. Assuming heat flows only in the cross-sectional plane can provide a useful and economical approximation for many welding situations. In particular, the results from a low cost cross-sectional analysis can be helpful in designing an efficient 3-D mesh. These three models are discussed in detail below.

E. *Two Dimensional Cross-Sectional Model*

A schematic diagram of the cross-sectional model is shown in Figure 4.[18] The double ellipsoid heat source (Figure 4(a)) is used to approximate the weld pool (cross section shown in Figure 4(b)). The heat input rate, $Q = \eta VI$ where V and I are the welding voltage and current, respectively, and η is the efficiency of the heat source, together with the ellipsoidal dimensions, define the distribution of power density in the heat source. A reference plane is established at some arbitrary position in the workpiece (Figure 4(c)). Associated with this reference plane is a FEM mesh with arbitrary thickness (Figure 4(d)). For each time increment the power density distribution is computed on the intersection of the reference plane and the ellipsoidal model. This power density distribution is projected throughout the thickness of the FEM mesh (Figure 4(d)). As the heat source moves through the reference plane, the temperature increases and then decreases. The temperature distribution in space can be represented with a series of slices as shown in Figure 7(a). Note that within a slice there is no temperature gradient in the x direction at any time in the cross-sectional model. The shape of the weld pool can be visualized as shown in Figure 7(b).

If it is assumed that $\partial T/\partial x = 0$ (see Figures 1 and 4), then every line parallel to x is an isotherm. Physically, this is a reasonable approximation for a strip heat source such as a sheet electron, laser beam, or a strip electrode in resistance welding. Even with wire electrode welds where the isotherms approximate distorted ellipsoids and the lines of constant x are clearly not isotherms, this model often predicts the thermal history of points with surprising accuracy for points sufficiently far from the heat source (Figure 8). The reason is that when isotherms are sufficiently elliptical, most of the heat flows perpendicular to the major axis of the ellipse. In fact, a one-dimensional model that assumes $\partial T/\partial x = 0$ and $\partial T/\partial z = 0$ often predicts the ther

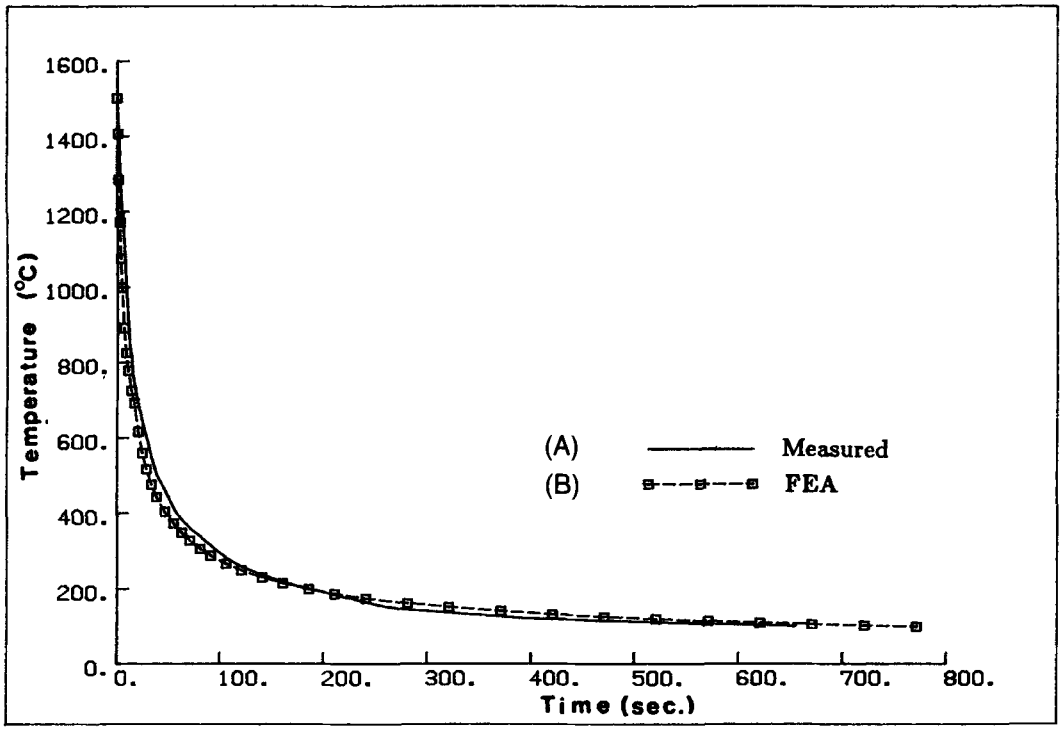

Fig. 8—Centerline (y = 0, Fig. 4) cooling curves: (A) experimental bead-on-plate weld (see Figs. 1 and 2), V = 30 volts, I = 265 amps, v = 3.81 mm/s, g (thickness) = 38 mm, T_0 = 20.5 °C. (B) FEA computed: ellipsoid parameters (see Fig. 4) a_1 = 9 mm, a_2 = 16 mm, b = 6 mm, c = 6 mm, thermal properties—see Figs. 4 and 5, combined radiation–convection surface heat transfer equation $h = 0.00241\varepsilon T^{1.61}$W/m^2 °C (Vinokurov[39]), arc efficiency η = 0.8 (shielded metal arc process).

mal history of a weld with considerable accuracy for points sufficiently far from the heat source. The accuracy of the cross-sectional model increases as the welding speed increases, the thermal diffusivity decreases, and locations farther from the heat source are considered. As these conditions are relaxed, the error in the model grows as the gradient $\partial T/\partial x$ increases and more heat flows in the x direction. Andersson attempted to assess this effect by comparing the analytic solutions for a one and two dimensional heat flow problem.[19] He argued that the results gave a qualitative estimate of the error that should be expected in the cross-sectional approximation to three dimensional reality. In this paper, the error is determined directly by comparing results from 3-D, in-plane, and cross-sectional models.

In this paper it is shown that the cross-sectional model is quite accurate for high speed production welds in steel and useful but subject to significant errors in high speed aluminum welds. However, in low speed aluminum welds or deep penetration EB welds the predicted FZ shapes are grossly in error (Figure 6(b)). At lower temperatures and greater distances from the heat source the model may still be considered acceptable. However, it cannot be used to analyze run-on or run-off effects.

Conceptually, this model is rather subtle. For the double ellipsoidal heat source model, the power density distribution is calculated on the intersection of the reference plane and the heat source. This power density distribution is then assumed to apply to a cross-sectional slice in which the heat flow is analyzed. The reference plane and the slice are different mathematical entities and should be clearly distinguished.

The cross-sectional analysis can be related to a 3D steady state analysis by mapping the cross-sectional temperatures, $T(x, y, t)$, onto a 3D steady state field, $T(x, y, \xi)$, where $\xi = x_0 - vt$, x_0 is the location of the arc at time zero and v is the arc speed in the direction x (Figures 1 and 7). This clearly illustrates the distinction between the reference plane and the cross-sectional slice. Thus the cross-sectional analysis is equivalent to a 3D steady state analysis in which heat flow is constrained to the reference plane; *i.e.*, $\partial T/\partial x = 0$. Clearly, coding a 3D FEM formulation for 3D steady state nonlinear heat transfer is expected to be both more accurate and computationally more efficient than the cross-sectional model. The reasons are that the heat flow need not be constrained to the reference plane and a 3D steady state problem is expected to require less computing than the 2D transient problem. However, the coding is non-trivial and the resulting equation set, $Kx = b$, is asymmetric. When it is coded, the authors expect it will make the cross-sectional model obsolete. Neither the cross-sectional nor 3D steady state analysis sheds any light on transient effects, such as weld starts or stops. Both are applicable only to infinite prismatic geometries, *i.e.*, geometries that could be extruded. The arc must move in the axial direction only. To deal with transient effects, an in-plane or 3D transient analysis is necessary. For these reasons, the authors have focused their attention on the 3-D transient formulation and neglected the 3-D steady state analysis.

F. *Two Dimensional In-Plane Model*

If it is assumed that $\partial T/\partial z = 0$ for a weld moving in direction x where z is the through thickness direction, a two

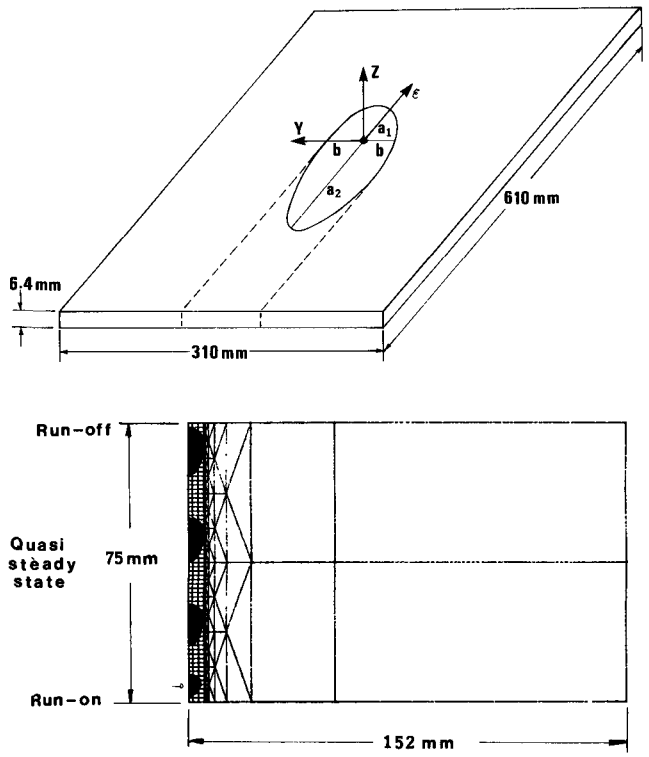

Fig. 9 — In-plane FEA of a thin plate (g = 6.4 mm) aluminum (Al-7003) weld showing how the weld pool expands from run-on size to the quasi-stationary state and expands again at run-off; welding process: gas metal arc weld (GMAW): V = 23.5 volts, 285 amps, 21.5 mm/s, T_0 = 20.5 °C; ellipsoid parameters a_1 = 3 mm, a_2 = 9 mm, b = 3 mm; thermal properties: temperature sensitive thermal conductivity and heat capacity taken from the data of Touloukian,[29] emissivity ε = 0.2,[53] and convection coefficient h = 12 W/m °C.[19]

dimensional in-plane model results (Figure 9). This model is accurate for full penetration EB welds *in vacuo* where every line parallel to z is an isotherm (Figure 6(b)). The error in the model grows as $\partial T/\partial z$ grows and more heat flows in the z direction. In most arc welds this model does not predict the FZ shape or size accurately. However, in some sense it projects or averages the three dimensional FZ onto the x-y plane and provides an estimate of the FZ size and shape. In sufficiently thin sheets or plates it does provide useful data for points at some distance from the weld pool (Figure 10). It permits variations in the geometry of the x-y plane such as that found in the Houldcroft test specimen to be analyzed accurately and economically. More importantly, the significant problem of weld starts and stops, of which repair welds and run-on and run-off welds are examples, can be analyzed (Figure 9).

G. *Three Dimensional Model*

A full three dimensional model with a sufficiently fine mesh can model the heat flow as accurately as errors in the material properties, geometry, heat input, convection, and radiation parameters permit. By repeating the analysis with various estimates of the data, error bounds for the computed temperatures can be estimated. The reason that three dimensional analysis has not been standard procedure for the thermal analysis of welds is simply that costs have not been affordable. Chapman[20] clearly documented the trend that computing hardware costs fall tenfold and the efficiency of numerical methods increases tenfold for a hundredfold fall in computing cost every seven years. The authors have demonstrated that a three dimensional analysis of a weld is now possible (Figure 10). It is quite likely that 3-D analysis will become standard practice by 1990.

The cost can be minimized by utilizing three dimensional elements near the heat source where three dimensional effects occur and a two dimensional in-plane approximation in regions farther from the heat source (Figure 11). The transition from the three to two dimensional model must be performed properly. Specifically, in the 2D mesh lines normal to the surface have constant temperatures. Therefore, the nodes in the 3D mesh at the transition that lie along such a line must be constrained to have constant temperatures and be coupled into the corresponding node in the 2D mesh to maintain compatibility. This is easily accomplished by applying sectorial symmetry to the transition nodes.[21]

In the two dimensional region the through thickness temperature gradient due to convection or radiation is ignored, of course. A cross-sectional analysis can be used to estimate the error and even more importantly identify the region requiring a three dimensional mesh.

H. *Spatial Discretization Requirements*

How fine must the finite element mesh be? How should the mesh be graded to achieve the desired accuracy while minimizing the cost in both mesh preparation and computing? It is cheap to prepare a very fine mesh that gives accurate results but with very high computing costs. It is more difficult to prepare a carefully graded mesh to achieve the desired accuracy with low computing costs. How to prepare meshes that satisfy both criteria is a question that will not receive a definitive answer for some years. The work of Kela, Voelcker, and Goldak[22] and Sheperd and Law[23] on fully automatic mesh generation lead this field.

However, some guidelines can be offered. The mesh must be sufficiently fine to model the heat source with adequate accuracy. Specifically, the Gaussian ellipsoidal model requires approximately four quadratic elements along each axis to capture the inflection of the Gaussian distribution. In Figure 12, a Gaussian distribution is approximated with 4, 8, and 30 quadratic elements across the function. Four elements provide a crude approximation and eight elements increase the accuracy considerably. With cubic elements, only two elements along an axis of the ellipsoid may be acceptable. Certainly one quartic element is much more accurate than two quadratic elements.

I. *Time Discretization Requirements*

The use of two point intergration in the time domain[24] implies linear interpolation. How long can the time steps be before the error becomes unacceptable? Figure 13 shows that approximately ten to twenty time steps are needed for the ellipsoidal heat source to cross the reference plane in the cross-sectional model. In the in-plane and three dimensional model, the heat source may move approximately one-half of a weld pool length in one time step.

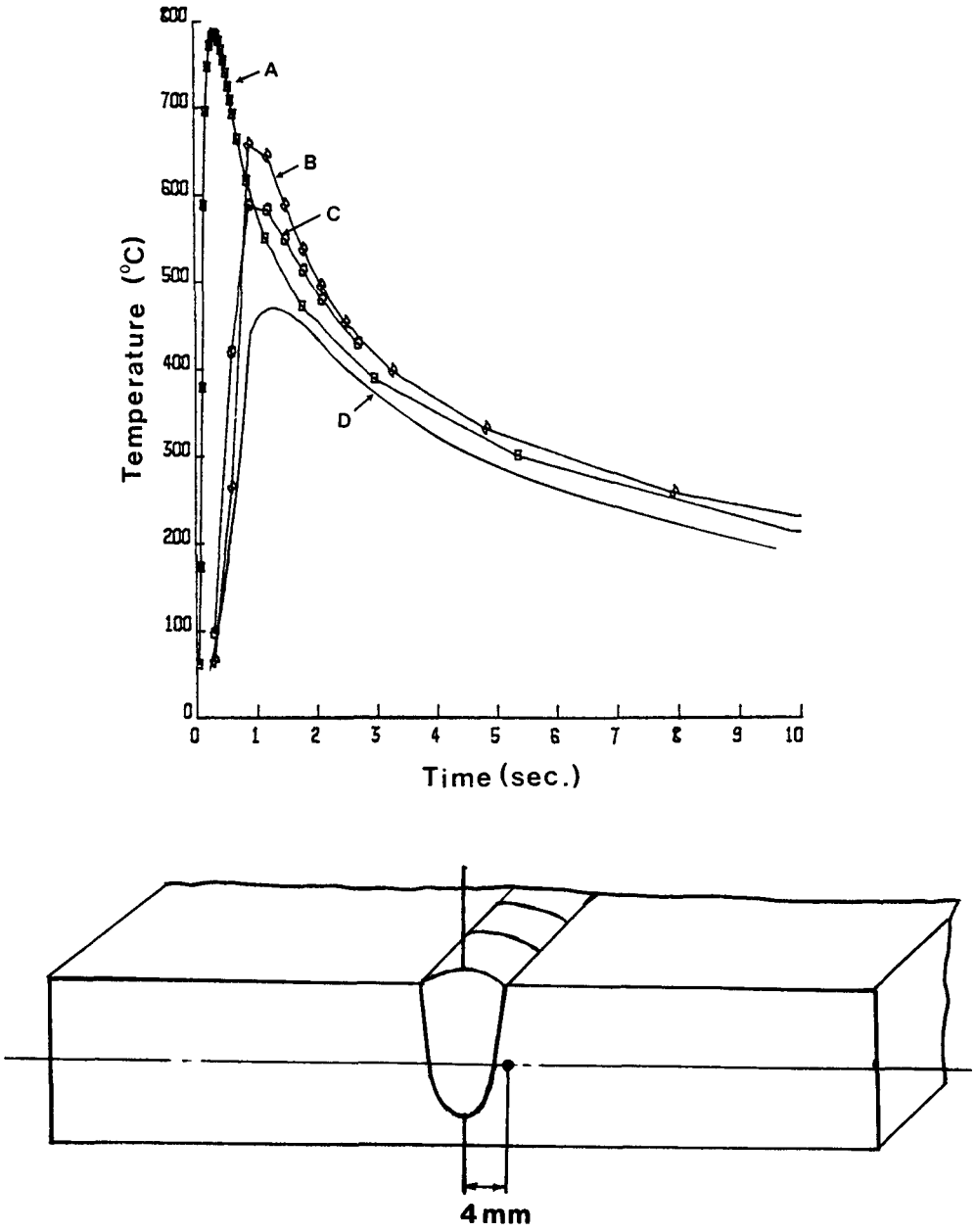

Fig. 10—FEA analysis of an aluminum weld: (A) cross-sectional model, (B) in-plane model, (C) full three-dimensional model, (D) experimentally measured time-temperature curve at 4 mm, mid-plane position; GMAW process: V = 23.5 volts, I = 285 amps, welding speed v = 21.5 mm/s, T_0 = 21 °C; computation parameters—thermal conductivity taken from the data of Touloukian,[29] emissivity ε = 0.2,[53] convection coefficient h = 12 W/m °C;[19] cross-sectional and three-dimensional ellipsoid parameters: a_1 = 3 mm, a_2 = 9 mm, b = 3 mm, c = 4 mm; in-plane ellipse parameters a_1 = 3 mm, a_2 = 9 mm, b = 3 mm.

It is important for the analyst to recognize the effect of interaction between the integration scheme: explicit (θ = 0), Crank-Nicholson (θ = 0.5), Galerkin (θ = ⅔), and implicit (θ = 1.0), and any prescribed thermal loads, fluxes, or power densities. The prescribed thermal loads, fluxes, and power densities are all converted to an equivalent nodal thermal load specified at the beginning of each time step and another at the end of each time step. The time integration scheme linearly interpolates these to the θ point. Several examples are shown in Figure 13. Any convective or radiative loads are computed at the θ temperature and added to the applied thermal load. This load can be considered to be applied for the full time increment.

Hughes[25] proved that the conductivity and capacitance matrices must be computed at the θ temperature in a nonlinear FEM analysis. Donea[26] showed that θ = ⅔ is more accurate than θ = 0.5 when high frequency components are present in the loads even though the respective convergence rates are linear and quadratic. The work of Pammer[27] should be consulted for a criterion for determining element size to analyze accurately rapid transients in surface temperatures.

J. *Nonlinear Material Properties*

The basic reference on high temperature heat transfer by Rohsenow[28] deals with measurement techniques in detail.

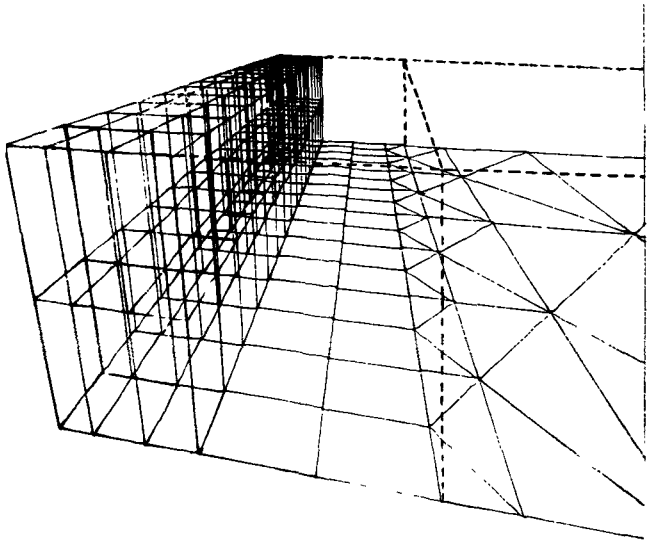

Fig. 11 — A representation of a three-dimensional mesh graded to a two-dimensional mesh where temperature changes are less severe. The dashed lines represent the physical dimensions of the workpiece being meshed in the 2-D region.

References 29 and 30 summarize much of the published high temperature data. Notwithstanding the above, the greatest limitation to computational weld mechanics is obtaining accurate temperature dependent material properties and models to predict properties as a function of history; *i.e.*, temperature, time, strain, *etc.* In general, properties depend on chemical composition, microstructure, and dislocation density. Therefore, they are dependent on the thermal history primarily through microstructural effects such as precipitation, transformations, annealing, recovery, *etc.* They are dependent on plastic strain history primarily through the density distribution of dislocations and vacancies. It would be desirable for manufacturers of materials to measure and publish basic thermal properties, because they should know their materials best and this would minimize wasteful duplication. The other possibility is that government laboratories assume this task. The analyst who

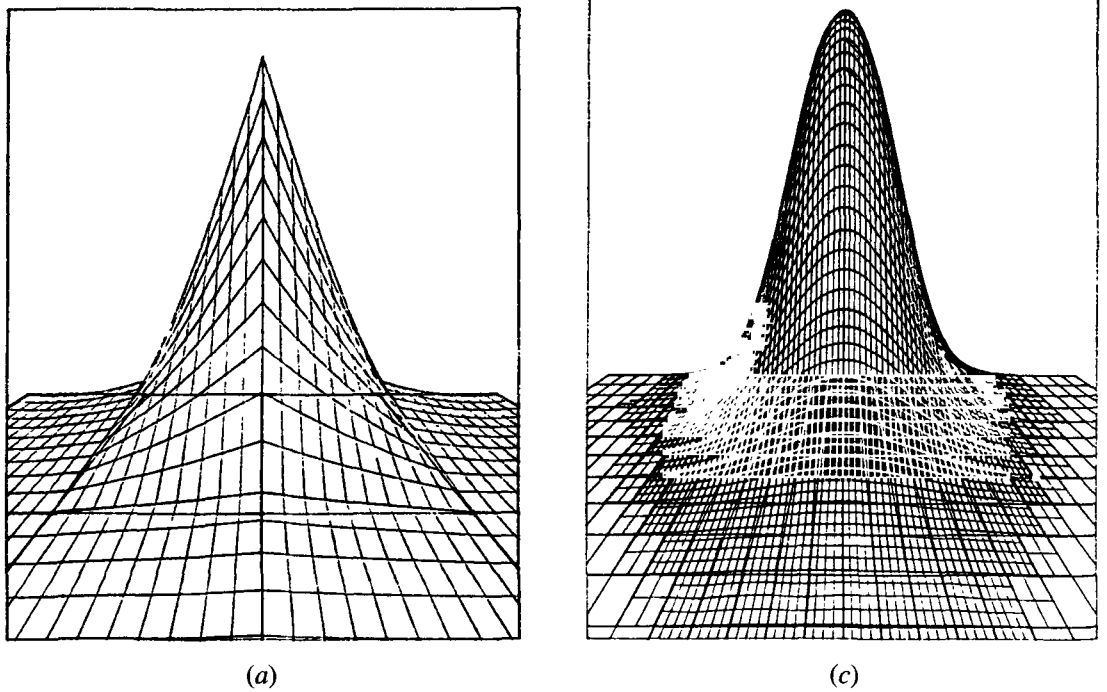

(*a*) (*b*) (*c*)

Fig. 12 — A pictorial representation of the double ellipsoid energy input distribution (cross-sectional) using (*a*) two elements, (*b*) four elements, and (*c*) many elements along the y-axis (Fig. 2). Note: four elements representing the double ellipsoid along any axis is considered sufficient.

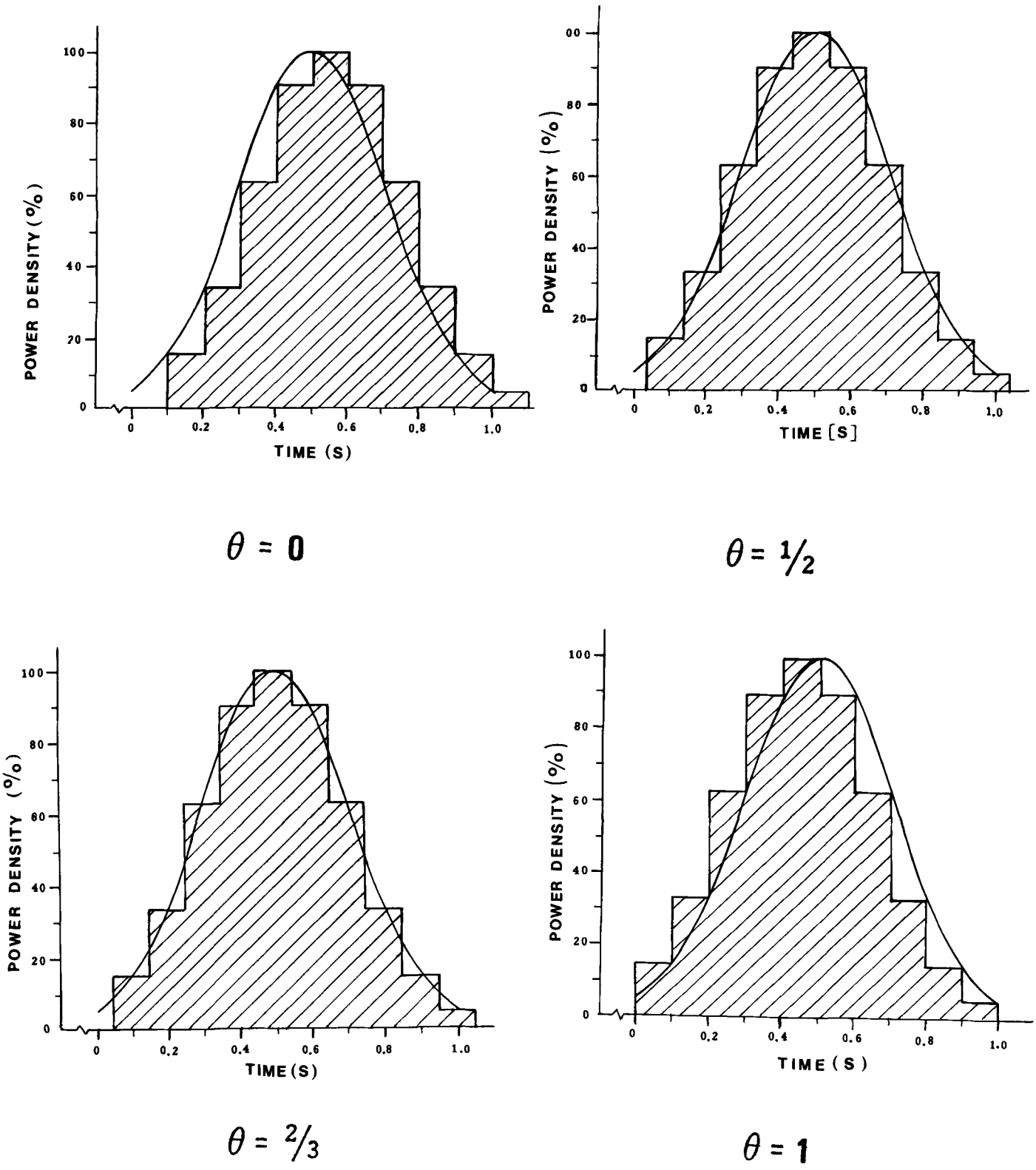

Fig. 13 — Variation of power density as a function of time as the heat source passes the reference plane in a cross-sectional FEA. The Gaussian energy distribution of a conical heat source as shown in Fig. 6 is represented in this diagram. It is clear that 10 to 20 time steps are required to integrate the distribution adequately.

fails to find the property data required must either have the data measured or use some estimate. The sensitivity of the results to the data can be checked by repeating the analysis with lower limit, best, and upper limit estimates of the data. However, if the analysis involves several properties, many analyses would be required to test all combinations. In this situation the analyst should consult an expert on the statistical design of experiments.

1. *Thermal conductivity*

Most thermal analyses of welds over the past forty years have assumed that the thermal properties were constant. In fact, Rosenthal's analysis cannot be extended to include nonlinear properties because the final transformation he applies is valid only for a linear equation. The thermal conductivity and volumetric specific heat of a 0.23 pct C steel are plotted as a function of temperature in Figures 2 and 3.[30] The temperature dependence is clearly substantial. An example of the error caused by assuming a temperature independent thermal conductivity and specific heat is shown in Figure 14. The values of constant thermal conductivity and specific heat chosen are those often recommended by advocates of Rosenthal's analytic solution. The error is clearly significant. Actually, the value of the thermal conductivity is frequently chosen to obtain the best agreement with welding experiments. For steels, the value of 25 W/m C is usually proposed for 3D heat flow and the value of 41 W/m C for 2D heat flow.[31] Clearly, these fictitious thermal conductivities are more correctly called undetermined coefficients that are used to match the equation to experimental data. Since the error in the flux for a given temperature gradient is directly proportional to the error in the thermal conductivity, it is desirable to use the best available data.

The cost of incorporating temperature dependent thermal conductivity in FEM codes is trivial and it should be used whenever the data are available. However, caution is necessary whenever the thermal properties are history dependent in addition to temperature dependent. The investigation of Farnia and Beck[32] is an important contribution in this area. They have shown that the thermal conductivity of aluminum 2024-T351 depends on the volume of precipitates. It appears that their methodology can be applied to other materials and other properties. As it now stands, the primary limitation is that it applies only to plates in the solution treated condition and deals only with precipitation. Nevertheless, this is a significant advance.

2. *Heat capacity and latent heats*

The heat capacity and enthalpy are related by:

$$\Delta H(T) = \int_{20}^{T} c_p(T)\, dT \qquad [9]$$

The temperature dependence of the heat capacity is usually incorporated into a FEM program by evaluating the capacitance matrix at the θ temperature.[33] This value of the heat capacity then applies for the entire duration of the time increment. In cases where the heat capacity varies rapidly as in ferrite near 700 °C (Figure 2), this can cause a significant error in a large time step. An alternative method uses an average value computed from the enthalpy, H, $c_p = (H_2 - H_1)/(T_2 - T_1)$ where the subscripts indicate that the enthalpy has been evaluated at the beginning and end of the time step. When $(T_2 - T_1) = 0$, care must be taken to avoid this technique and simply use the temperature dependent value of $c_p(T)$. Of course, small time steps should be considered to achieve the desired accuracy.

Transformations, such as melting and the ferrite-austenite transformation in steel, are more difficult to analyze rigorously. The transformation surface, *e.g.* the liquid-solid boundary, has a discontinuity in the thermal gradient which moves. During melting the latent heat is absorbed. During freezing the latent heat is released. Since this latent heat in steel is 2.1×10^9 J/m^3 and the specific heat is 4.5×10^6 J/m^3 C, the transformation absorbs as much heat as a temperature change of 470 °C. Solid-solid transformations have less effect on the temperature field, but because they can affect the cooling rate substantially during transformation (Figure 15), the microstructure can be altered significantly.

The simplest method of including the latent heat is to compute the specific heat from the enthalpy as discussed above. A better way is contained in the presentation of Rolphe and Bathe.[34] Whenever a nodal temperature crosses a transformation temperature, this is noted together with whether it is cooling or heating. A volume or mass is associated with each node and the corresponding heat of transformation, J, is computed. If a node transforms, the temperature is reset to the transformation temperature and the heat subtracted from the heat of transformation until it is reduced to zero. At that time the node is set free. In all other respects, it is a standard FEM analysis. The algorithm is simple, relatively easy to code, and efficient.

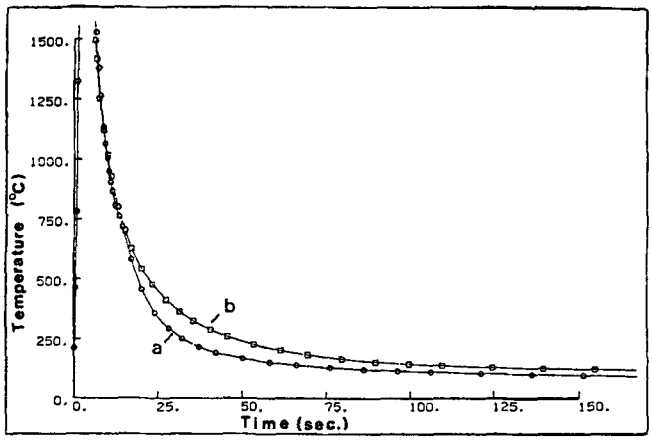

Fig. 14—Effect of thermal properties on the FEA computed weld cooling curve of a steel weld: (*a*) variable thermal properties (Figs. 2 and 3), (*b*) constant thermal properties k = 25 W/m °C, $C\rho = 6 \times 10^6$ J/m^3 °C. Weld parameters described in Figs. 4 and 8.

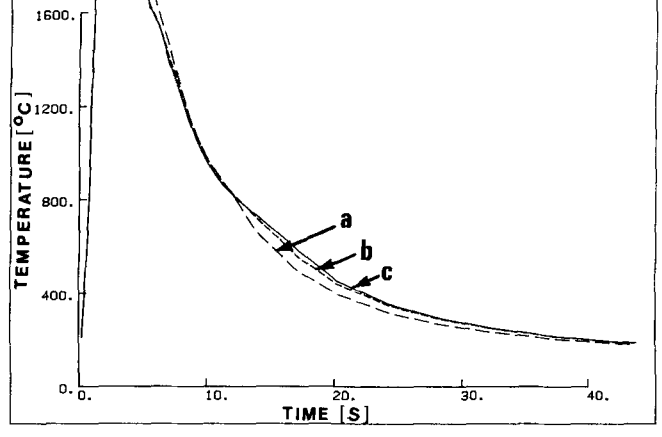

Fig. 15—The time-temperature centerline thermal history for a steel weld (see Fig. 4 for welding conditions) without latent heats of fusion and transformation (curve a), with latent heat of fusion included (curve b), and with both latent heat of fusion and transformation included (curve c). Note the substantial effect due to the latent heats of transformation.

The most accurate method of dealing with latent heats of transformation have been developed by Blanchard and Fremont for analyzing frozen soils where the latent heat is the dominant effect and accuracy is critical.[35] However, this algorithm, which can compute two phase regions or mushy zones, is more complex.

3. *Precipitation and solution effects*

Although the effect of precipitates on mechanical properties is well understood and documented, relatively little data exist for the effect of precipitates on thermal properties. The thermal conductivity in 2024-T351 is a function of the volume of precipitates. In aluminum 2024 alloys, the thermal conductivity is lowest when the copper is in solid solution and highest when the copper is in the precipitate particles. Farnia and Beck[32,36] have presented equations for computing the thermal conductivity of aluminum 2024-T351 during a thermal cycle. They proposed the following equations:

$$k(T,t) = k_0(T) + [k_m(T) - k_0(T)]\frac{\eta(T,t)}{\eta_m(T)} \quad [10]$$

where

$$\eta_m(T) = 8.68 \times 10^{-2} + 3.59 \times 10^{-3} T \quad [11]$$

$$k_m(T) = 148.2 + 0.1115T \quad [12]$$

$$k_0(T) = 73.2 + 0.3725T \quad [13]$$

$$\frac{\partial \eta(T,t)}{\partial t} = \frac{1}{\tau(T)}[\eta_m(T) - \eta(T,t)] \text{ if } \eta_m(T) > \eta(T,t) \quad [14]$$

$$\tau(T) = \exp\left(-31.93 + 15.7\frac{1000}{T + 273}\right) \quad [15]$$

$k(T,t)$ = the thermal conductivity at temperature T (C), and time t (s).
$k_0(T)$ = the thermal conductivity at temperature T (C) for precipitate free 2024.
$k_m(T)$ = the thermal conductivity at temperature T (C)with maximum precipitation at this temperature.
$\eta_m(T)$ = maximum volume fraction of precipitate at temperature T.
$\eta(T,t)$ = volume fraction of precipitate at temperature T and time (t).
$\tau(t)$ = a time constant characterizing the rate of precipitation at temperature T.

It is a straightforward matter to incorporate these data and behavior into a FEA program to predict the volume fraction of precipitate and the precipitation dependent thermal conductivity. There is a clear need to extend this method to begin with any microstructure and to account for the solution or coarsening of precipitates.

Ashby and Easterling[37] predicted austenite grain growth in the HAZ of Nb and V microalloyed steels due to the dissolution of NbC and VC. Ion and Easterling[38] have extended this work to TiC precipitates. Here the austenite grain growth in the HAZ was due to Ostwald ripening of TiC. Both papers predicted only the final austenite grain size. Although their model does not predict the grain size or volume fractions of precipitate as a function of time and temperature, it is an important step toward this goal. At this point in time this work has not yet been extended to thermal properties. However, predicting microstructural changes that occur is an important first step and it is not difficult to imagine that algorithms for computing thermal conductivity similar to the Farnia/Beck approach will appear in the future.

4. *Convection and radiation*

Given the heat transfer coefficient, h, convective heat transfer is easily included in the FEM analysis. Newton's equation for cooling, which may be taken as the definition of the heat transfer coefficient, is $q = h(T - T_{amb})$. The value of h must be measured experimentally or taken from handbooks which are based on experiment. Based on experimental data, Vinokurov suggests the following equation for welding hot rolled steel plates.[39] This equation includes both radiation and convection effects:

$$h = 24.1 \times 10^{-4}\, \varepsilon T^{1.61} \text{ (W/m}^2\text{ C)} \quad [16]$$

In the authors' experience, this equation is not as accurate as applying both Newton's equation for cooling and the Stefan-Boltzmann equation for radiation with appropriate coefficients.

Radiation losses from the molten zone can be quite different from the Vinokurov relationship. This could have a considerable effect on the size of the molten pool. However, since the radiation losses from the molten pool are included in the "weld efficiency", the authors do not compute radiation losses from the molten pool. Far from the heat source, heat flow can be convection dominated if the workpiece and fixturing are not so large that the temperature rise in the workpiece is negligible.

In radiative heat transfer the emissivity must be measured experimentally. In exceptional situations, it may be desirable to take into account view factors. The analysis of an electron beam cavity is an example. If a laser beam interacts with its plume, a participating media should be considered. Neither view factors nor participating medium are considered in this paper.

5. *Errors in the computed and measured temperature fields*

Sufficent data now exist to state that temperatures, $T(x,y,z,t)$, can be computed accurately by FEA for welds in steels (Figure 8). However, more research is needed to establish appropriate models and their accuracy for welds in aluminum alloys where precipitation effects are significant. For example, it is not clear whether the computed or measured temperatures shown in Figure 10 are more accurate. In a discussion of errors in $T(x,y,z,t)$, three distinct welds should be recognized. First, the weld described by the experimental data, the weld computed by FEA, and the real weld. Both the experimental data and the FEA results are in error. The issue is to determine the sources of the error. In the FEA the uncertainty in the efficiency of the GMAW process is high. In this analysis it was taken as 65 pct. The temperatures are measured with thermocouples pressed into a hole. An error of 0.5 mm in positioning the thermocouple can cause an error of 25 °C in peak temperature in this particular situation. Weld data must be measured more accurately and more research done on computer models in order to compute accurately the temperatures in welding aluminum.

III. APPLICATIONS AND FURTHER RESEARCH

The reader may well ask how this theory can best be exploited. The most obvious application is to compute the temperature field in a specific welding situation with given welding current, voltage, speed, geometry, and thermal properties. These data could then be used to compute the distortion (residual strain) and residual stress as Patel[40] has done. In the longer term the method of Hellen could be used to compute the fracture strength[41,42] and the method of Kalev[43] to compute the fatigue life of a welded structure.

An important extension of the present work would be to determine correlations between heat source model parameters such as ellipsoid dimensions and welding parameters such as current, voltage, and speed. The work of Christensen[14] and Bibby *et al.*[15] on nondimensional fusion zone sizes is in this spirit. The work of Key, Smartt, Chan, and McIlwain[17] on the effect on bead morphology of changes of welding current, speed, and filler wire speed in GTAW welds provides an excellent starting point for such research.

If such correlations can be developed, then FZ size and shape could be computed prior to experiment.[16] Welding procedures and the design of welded structures could be optimized by computer without ever striking an arc. When this happens, the authors predict that lead times, development costs, reject, and rework costs will be reduced dramatically.

In the longer term the correlation between the welding parameters and the heat source model parameters could be computed by developing models for the fluid mechanics of the weld pool and the magnetohydrodynamics of the arc. Until such models are developed, our knowledge and understanding of stirring in the weld pool, weld pool surface shape, and the physics of the arc will remain rudimentary.

The application of temperature fields to compute the distortion (residual strain) and the residual stress in the weld will be described in a later publication.[44]

REFERENCES

1. R. R. Rykalin: *Welding in the World*, 1974, vol. 12, No. 9/10, pp. 227-48 (Houdrement Lecture, International Institute of Welding, London, 1974, pp. 1-23).
2. *The Physics of Welding*, J. F. Lancaster, ed., Pergamon Press, 1984, pp. 1-293.
3. A. H. Dilawari, J. Szekely, and T. W. Eagar: *Metall. Trans. B*, 1978, vol. 9B, pp. 371-81.
4. A. H. Dilawari, T. W. Eagar, and J. Szekely: *Welding Journal*, January 1978, pp. 24-30.
5. S. Lawson and H. Kerr: *Welding Research International*, 1976, vol. 6, No. 5, 6.
6. D. Rosenthal: *Trans. ASME*, 1946, vol. 68, pp. 849-65.
7. P. S. Myers, O. A. Uyehara, and G. L. Borman: *Welding Research Council Bulletin*, New York, NY, 1967, No. 123.
8. O. Westby: Report, Department of Metallurgy and Metals Working, The Technical University, Trondheim, Norway, 1968.
9. Z. Paley and P. D. Hibbert: *Welding Journal Research Supplement*, 1975, vol. 54, pp. 385s-92s.
10. V. Pavelic, R. Tanbakuchi, O. A. Uyehara, and P. S. Myers: *Welding Journal Research Supplement*, 1969, vol. 48, pp. 295s-305s.
11. S. Kou: *Metall. Trans. A*, 1982, vol. 13A, pp. 363-71.
12. J. H. Argyris, J. Szimmat, and K. J. Willan: *Computer Methods in Applied Mechanics and Engineering*, 1982, vol. 33, pp. 635-66.
13. J. A. Goldak, A. Chakravarti, and M. J. Bibby: *Trans. AIME*, June 1984, vol. 15B, pp. 299-305.
14. N. Christensen, L. de.V. Davies, and K. Gjermundsen: *British Welding Journal*, 1965, vol. 12, pp. 54-75.
15. M. J. Bibby, G. Y. Shing, and J. A. Goldak: *CIM Metallurgical Quarterly*, Jan. 1985, in press.
16. A. P. Chakravarti, J. Goldak, and A. S. Rao: *Thermal Analysis of Welds*, International Conference on Numerical Methods in Thermal Problems, Swansea, U.K., Nov. 1985.
17. J. F. Key, H. B. Smartt, J. W. Chan, and M. E. McIlwain: *Welding Technology for Energy Applications*, Proceedings International Conference, Gatlinburg, TN, 16-19 May, 1982, compiled by S. A. David and G. M. Slaughter, pp. 179-99.
18. E. Friedman: *Journal Pressure Vessel Technology*, Trans. ASME, 1975, vol. 97, pp. 206-13.
19. B. A. B. Andersson: *Journal of Engineering Materials and Technology*, Trans. ASME, 1978, vol. 100, pp. 356-62.
20. D. R. Chapman: *AIAA Journal*, December 1969, vol. 17, No. 12, pp. 1293-1313.
21. B. M. Irons and S. Ahmad: *Techniques for Finite Elements*, Ellis Horwood, West Sussex, U.K., 1980.
22. A. Kela, H. Voelcker, and J. A. Goldak: International Conference on Accuracy Estimates and Adaptive Refinements in Finite Element Computations (ARFEC), Sponsored by the International Association of Computational Mechanics, Lisbon, Portugal, June 19-20, 1984.
23. M. S. Sheperd and K. H. Law: International Conference on Accuracy Estimates and Adaptive Refinements in Finite Element Computations (ARFEC), Sponsored by the International Association of Computational Mechanics, Lisbon, Portugal, June 19-20, 1984.
24. O. C. Zienkiewicz: *The Finite Element Method*, McGraw-Hill Book Company, New York, NY, 3rd ed., 1977.
25. T. J. R. Hughes: *Computer Methods in Applied Mechanics and Engineering*, 1977, vol. 10, pp. 135-39.
26. J. Donea: *International Journal for Numerical Methods in Engineering*, 1974, vol. 8, pp. 103-10.
27. Z. Pammer: *International Journal for Numerical Methods in Engineering*, 1983, vol. 15, pp. 495-505.
28. W. M. Rohsenow and J. P. Hartnet: *Handbook of Heat Transfer*, McGraw-Hill, New York, NY, 1973.
29. Y. S. Touloukian, Powell, Ho, and Klemens: *Thermal Conductivity: Metallic Elements of Alloys*, Plenum Publishing Co., New York, NY, 1970.
30. *Physical Constants of Some Commercial Steels at Elevated Temperatures*, The British Iron and Steel Research Association, London, Butterworths Scientific Publications, 1953.
31. N. Yurioka, S. Ohsita, and H. Tamehiro: The Specialist Symposium on Pipeline Welding in the 80's, Melbourne, Australia, March 18/81.
32. K. Farnia and J. V. Beck: *Journal of Heat Transfer*, Trans. ASME, vol. 99, pp. 471-78.
33. G. Comini, S. del Guidice, R. L. Lewis, and O. C. Zienkiewicz: *IJNME*, 1974, vol. 8, pp. 613-24.
34. W. D. Rolphe, III and K. J. Bathe: *IJNME*, 1982, vol. 18, pp. 119-34.
35. D. Blanchard and M. Fremont: *IJNME*, 1984, vol. 20, pp. 757-71.
36. S. Al-Araji and J. V. Beck: *Journal of Heat Transfer*, Trans. ASME, 1975, pp. 148-49.
37. M. F. Ashby and K. E. Easterling: *Acta Metall.*, 1982, vol. 30, pp. 1969-78.
38. J. C. Ion and K. E. Easterling: The Third Scandinavian Symposium in Materials Science, 20-21 June, 1983, The University of Oulu, Finland, Metal Abstracts 8407-72-0526.
39. V. A. Vinokurov: *Welding Stresses and Distortions*, The British Library, Lending Division, Translated from Russian into English by J. E. Baker, 1977, pp. 118-19.
40. B. Patel: Ph.D. Thesis, Carleton University, Ottawa, ON, Canada, Jan., 1985.
41. T. K. Hellen: *IJNME*, 1983, vol. 19, pp. 1713-37.
42. T. K. Hellen: *IJNME*, 1975, vol. 9, pp. 187-97.
43. I. Kalev: *Computers and Structures*, 1981, vol. 13, pp. 709-16.
44. B. Patel, J. A. Goldak, and M. J. Bibby: Carleton University, Ottawa, ON, Canada, unpublished research, 1985.